Hindawi
Advances in Civil Engineering
Volume 2019, Article ID 8390345, 13 pages
https://doi.org/10.1155/2019/8390345

Research Article

Experimental Investigation on the Effect of Steel Fibers on the Flexural Behavior and Ductility of High-Strength Concrete Hollow Beams

Ahmmad Abbass,[1,2] **Sallal Abid**,[3] **and Mustafa Özakça**[1]

[1]*Department of Civil Engineering, Gaziantep University, Gaziantep, Turkey*
[2]*Southern Technical University-Shatrah Technical Institute, Basra, Iraq*
[3]*Department of Civil Engineering, Wasit University, Kut, Iraq*

Correspondence should be addressed to Sallal Abid; sallal@uowasit.edu.iq

Received 4 October 2018; Revised 4 December 2018; Accepted 11 December 2018; Published 15 January 2019

Academic Editor: Lukasz Sadowski

In this study, an experimental work was directed toward comparing the flexural behavior of solid and hollow steel fiber-reinforced concrete beams. For this purpose, eight square cross-sectional beam specimens, four solid and four hollow, were prepared. One concrete mixture with four different steel fiber contents of 0, 0.5, 1.0, and 1.5% were used. The side length of the central square hole was 80 mm, whereas the cross-sectional side length was 150 mm. All beams were tested under four-point monotonic loading until failure. In addition to the solid and hollow beams, cylinders were cast to evaluate the compressive strength, splitting tensile strength, and modulus of elasticity, whereas prisms were used to conduct the fracture test. The test results showed that all fibrous beams failed in flexure, whereas those without fiber exhibited flexural-shear failure. In general, the flexural behavior of fibrous-beams was superior to that of beams without fiber. The hollow beams with fiber contents of 0, 0.5, and 1.0% were observed to withstand lower loads at cracking, yielding, and peak stages compared with their corresponding solid beams; this was not the case for the 1.5% fiber hollow beam, which exhibited a higher peak load than its corresponding solid beam. Although all eight beams exhibited ductility indices higher than 3.7, hollow beams exhibited better ductility than solid beams, showing higher ductility index values.

1. Introduction

With the quick and huge development of the construction industry across the world, the demand for concrete has increased significantly over the last two decades. This is attributed to the attractive characteristics of concrete, including its high compression capacity, the availability of its constituents, and the ease of its production, in addition to the production cost, which is moderately satisfactory for such developments. However, one of the serious defects of concrete is its low capacity to withstand tensile stresses. Therefore, structural members such as foundations, columns, slabs, and beams are made of concrete reinforced with steel reinforcing bars.

In recent decades, the use of discrete short fibers was introduced as a solution to enhance concrete tensile strength. Several metallic and synthetic types of fibers can be used for this purpose. However, the most focus was on the use of steel fibers, which have high tensile strength and proven crack bridging potential. Such characteristics of the steel fiber can be used to alter the brittle behavior of concrete under tensile stresses to a more ductile behavior. Steel fiber-reinforced concrete was also proven to be much more ductile than normal concrete under seismic and impact loads. Several experimental studies were conducted during the last decades to investigate the mechanical properties of steel fiber-reinforced concrete [1–6], whereas many other studies were focused on the effect of the use of steel fiber to enhance

the flexural performance of unreinforced [7–11] and reinforced [12–23] concrete beams.

One of the serious disadvantages of reinforced concrete is the heavy weight of such a type of construction material. Consequently, more loads and thus more bearing stresses are transferred to the soil, which urges the use of larger and may be deeper foundations. As a result, the cost would be increased. Several solutions were proposed by researchers to reduce the effect of concrete heavy weight. Among these solutions to reduce the weight of the structure are the use of lightweight aggregates and the use of composite materials and structures, and the use of recycled aggregates was suggested to reduce the construction cost [24, 25]. The use of optimized structural sections can also be considered as a candidate solution. Hollow sections are types of optimized structural sections that reduce the cross-sectional size of structural members, leading to a reduced weight and lower consumption of concrete materials. Thus, compared with solid sections, hollow ones can be considered lighter and more economical. Although the reduction in section means lower moment of inertia, which may lead to lower strength and higher deformations, the use of steel fibers is known to increase the flexural strength and enhance the flexural behavior of reinforced concrete beams. Hence, this positive contribution may substitute the reduction in strength and performance resulting from the reduction of the section size of hollow beams compared with solid ones.

Few experimental research studies were found in the literature on the flexural behavior of reinforced beams with longitudinal holes [26–28]. Altun et al. [26] tried to evaluate the flexural behavior of box steel fiber-reinforced concrete beams. Normal strength concrete of 22 MPa compressive strength and 60 mm length steel fibers with a maximum dosage of 60 kg/m^3 (0.77% V_f) were used. They showed that a 44% reduction in weight can be obtained but with a 29% lower load carrying capacity. Murugesan and Narayanan [27, 28] experimentally investigated the flexural behavior of reinforced concrete beams having a small-sized longitudinal circular hole (5% of cross-sectional area). They showed that the load carrying capacity of hollow beams reduces as the hole size increases and it was in general lower than that of solid beams. Moreover, they observed that the deflection increases as the hole size increases.

The previous review shows that hollow beams can be considered as a candidate solution to reduce the weight of the structure and to provide a more environment-friendly solution. However, research works to evaluate the flexural behavior of hollow beams are very limited in the literature. Moreover, the beams of the few research studies found in the literature were either reinforced with limited amount of steel fiber or have no fibers and were all made of moderately low compressive strength concrete. Trying to fill some gaps of knowledge about this issue, in this study, an experimental work was directed toward investigating the flexural performance of high-strength steel fiber-reinforced hollow concrete beams. For this purpose, a square central longitudinal hole was used to reduce the cross-sectional area by approximately 28% and steel fiber contents up to 117 kg/m^3 were incorporated in the concrete mixtures.

2. Experimental Work

2.1. Concrete Mixture and Material Properties. Solid and hollow beams with high strength concrete and reinforced with steel fibers and conventional steel bars were produced to conduct the experimental work of this study. A previously used high-strength concrete mixture was adopted [29] to achieve a 28-day cylinder compressive strength (f'_c) of 60 MPa. Table 1 lists the details of the adopted mixture, in which the proportions of all materials were fixed except the dosage of steel fiber. In this study, cold drawn glued hooked-end steel fibers were adopted with three volumetric contents of 0.5, 1.0, and 1.5%. The use of high steel fiber V_f (more than 1.5%) decreases the workability and increases the opportunity of fiber balling in the presence of aggregate (sand and gravel), which results in lower compressive strength. Therefore, a 1.5% hooked-end steel fiber was suggested as an effective and economical volume fraction [30]. Katzer et al. [31, 32] clearly indicated that hooked-end steel fiber is the most popular and effective type of reinforcing fiber for concrete. The diameter, length, and aspect ratio of the used steel fiber were 0.55 mm, 30 mm, and 55, respectively, wheras its density and tensile strength were 7800 kg/m^3 and 1500 MPa, respectively. Crushed stone with a maximum diameter of 10 mm was used as coarse aggregate. Natural sand was used as fine aggregate. More details about the used materials are listed in a previous work [29]. The used cement was Portland cement type 42.5R, whereas silica fume was used as partial cement replacement. The use of silica fume is known to positively affect the mechanical properties of concrete because of its effective reaction with the cement components [33–35]. To assure an acceptable workability, the high range water reducer Master Glenium 51 was used in all mixtures. Twenty-four hours after concrete casting, the beams and control specimens were removed from their molds and cured in temperature-controlled water tanks for 28 days.

2.2. Control Tests. Three control tests were adopted to evaluate the strength and elasticity of the prepared concrete mixtures. The concrete compressive strength, splitting tensile strength, and modulus of elasticity were evaluated using 100×200 mm cylinders in accordance with ASTM C39, ASTM C496, and ASTM C469, respectively. In addition to the abovementioned three control tests, three-point flexural tests were conducted using $100 \times 100 \times 500$ mm concrete beams. According to RILEM FMC-50, the beams were notched at the centerline of the bottom surface to perform the fracture energy test [36], yet the test span was different. The notch depth was 40 mm, whereas the test span was 400 mm for all tested beams. The flexural tests were conducted using an electromechanical closed-loop servo-controlled universal testing machine from INSTRON with a capacity of 250 kN. The test setup and the details of the test specimens are shown in Figure 1. The performed tests were displacement controlled at a rate of 0.2 mm/min.

Table 1: Details of concrete mixtures [29].

Mix code	Steel fiber		Cement (kg/m^3)	Coarse aggregate (kg/m^3)	Sand (kg/m^3)	Silica fume (kg/m^3)	HRWR (kg/m^3)	W/C	Slump (mm)
	V_f%	kg/m^3							
B0.0	—	—	465	680	1170	35	6.6	0.43	105
B0.5	0.5	39.3					6.7		77
B1.0	1.0	78.5					6.7		69
B1.5	1.5	117.8					6.8		63

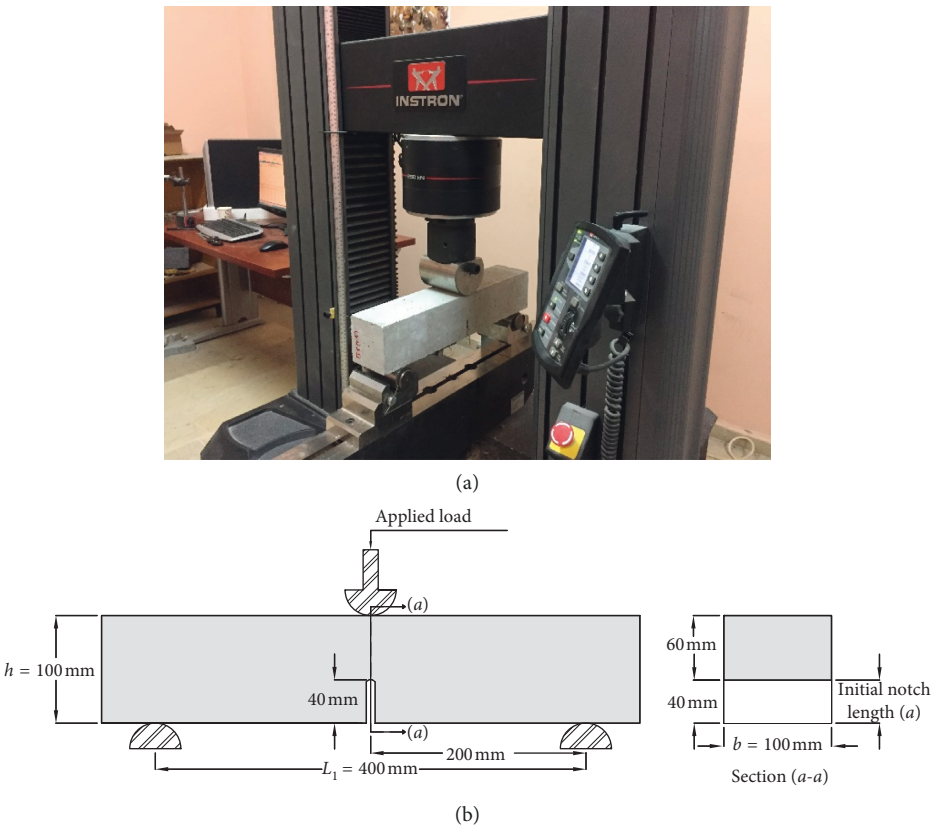

Figure 1: Specimen geometry and test setup for fracture energy.

2.3. Hollow Reinforced Concrete Beams. To investigate the effect of sectional hollowing on the flexural performance of steel fiber-reinforced beams, a total of 8 beams were cast. All beams have a square cross section with a side length of 150 mm and a beam length of 850 mm. The flexural tests of all beams were conducted under four-point loading with a span of 750 mm where the midspan deflection was measured using one linear variable differential transformer (LVDT), as shown in Figure 2. From the literature [37], it was observed that an a/d ratio of 2.5 resulted in the lowest flexural capacity, whereas the highest flexural capacity was attained with an a/d ratio of 1.5. In this research, all beams were tested using the same test configuration and with a fixed shear arm to effective depth ratio (a/d) of 2.0. Thus, the effect of a/d was kept constant, where for beams with the same materials and dimensions but with different a/d values, the flexural strength and behavior varied considerably.

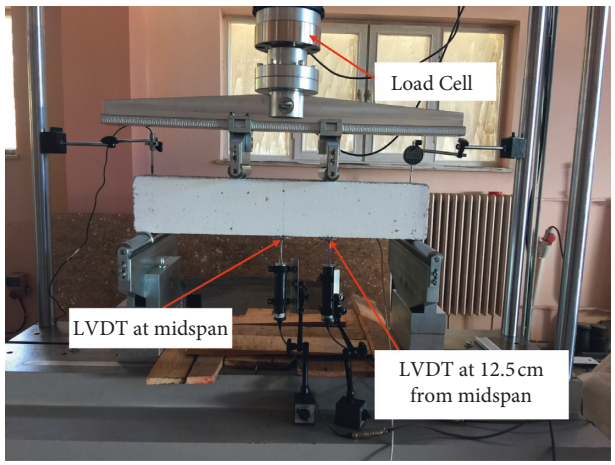

Figure 2: Test setup of the solid and hollow beams.

The experimental program was directed toward investigating the effect of cross-sectional hollowing and the dosage of the steel fiber. The hole of hollow beams was square with its center coinciding with the center of the beam cross section. Thus, the thicknesses of the top, bottom, and side walls were equal. The hollow beams were manufactured with a hole side length of 80 mm; thus, the wall thickness was 35 mm. As a result, the cross-sectional area of the hollow beams was 28.4% less than that of solid beams. All beams were reinforced with 8 mm steel reinforcing bars, as shown in Figure 3. It is clear that the wall thickness is slightly larger than the steel fiber length, which has less preferential fiber alignment compared to solid beams [38–40]. Such size may also lead to concrete casting difficulties. Therefore, the concrete was carefully cast in the mold in stages. Firstly, the bottom flange was poured with external vibration, and then the remaining walls were cast. The tested beams were divided into two groups. The first group consisted of four solid beams (S) with different fiber contents of 0, 0.5, 1.0, and 1.5%, whereas the second group consisted of four hollow beams (H) with the same sequence of fiber contents. The beam identification number starts with letters S or H, followed by the fiber content. Thus, the identification number of a hollow beam with 1.5% fiber content becomes H-1.5 and so on. All beams were cast with a fixed number of stirrups to assure flexural failure. Figure 3 shows the geometry and reinforcing details of the beams tested in this study.

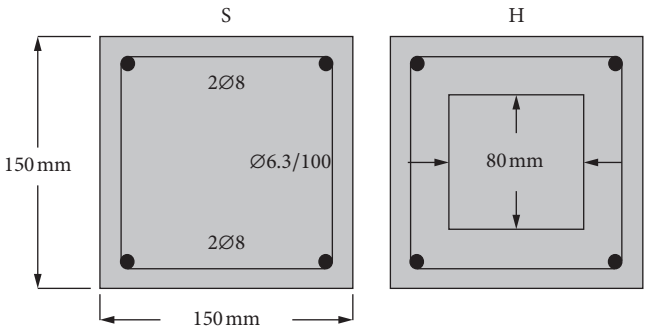

Figure 3: Sectional geometry and reinforcing details of the solid and hollow beams.

Table 2: Fiber volume fraction and control test results of the four mixtures.

Mix code	V_f		f'_c	f_{sp}	E
	%	kg	MPa	MPa	GPa
B0	0.0	0	63.3	4.2	36.04
B0.5	0.5	39.2	61.7	5.4	35.79
B1.0	1.0	78.5	73.3	6.4	37.70
B1.5	1.5	117.7	73.4	6.6	36.78

3. Results of Control Tests

The test results of the control cylinders show that inclusion of 1.0 and 1.5% of steel fiber resulted in obvious enhancement in compressive strength, whereas the 0.5% steel fiber content was ineffective. From the comparison between the compressive strengths of the 1.0% and 1.5% steel fiber, it is obvious that both fiber contents resulted in almost identical strength values. The percentage increase of compressive strength was approximately 16% for fiber contents of 1.0 and 1.5%. For the same contents of steel fibers, Song and Hwang [2] reported an increase of 15%, which agrees well with the results of the current research. Abbass et al. [5] reported a maximum development of 8%, which is consistent with the results obtained by Thomas and Ramaswamy [3] for cube and cylinder specimens (2.6% to 8.3%) for 1.5% fiber content. On the other hand, other researchers [11, 26] reported insignificant drop or increase in compressive strength of steel fiber reinforced concrete (SFRC). Table 2 summarizes the experimental results of the mechanical properties of the controlling mixes.

The test results also showed that the splitting tensile strength increases with the increase in fiber content, which is frequent in the literature [41–44]. The increase in splitting tensile strength can easily be attributed to the fiber bridging potential of tensile cracks. Comparing the results, it is obvious that the splitting tensile strength increased by approximately 30% when only 0.5% steel fiber was included, whereas this increase jumped to approximately 52% for fiber content of 1.0% and 57% for fiber content of 1.5%. Ashour et al. [14] reported that, for concrete with 79 MPa compressive strength and 1.0% steel fiber content, the splitting tensile strength increased by 52%, which completely agrees with the current results, whereas Thomas and Ramaswamy [3] reported an increase of 41% for a similar concrete grade. On the other hand, it was found out that there is no clear trend for the results of the modulus of elasticity, which reveals that the inclusion of steel fiber is not so effective (Table 2).

4. Results of Fracture Energy Test

The fracture energy (G_F) of a prism tested under flexure can be defined as the energy required to crack a unit area, which is determined from the load-deflection curve of the tested prism. In the current investigation, the fracture test recommended by RILEM FMC-50 [36] was adopted. From the three-point flexural test and using the central deflection, in addition to mass and geometry, of the tested prism, the following equation was used to calculate the fracture energy G_F:

$$G_F = \frac{W_0 + m \times g \times (L_1/L) \times \delta_f}{b \times (h - a)}, \quad (1)$$

where the prism geometrical parameters b, h, a, and L_1 are shown in Figure 1, L is the length of the specimen, m is the specimen mass, g is the gravity acceleration, and δ_f is the central displacement (deflection) at failure.

Considering the modulus of elasticity of concrete E_c and its tensile strength f_t and to evaluate the brittleness of concrete using the tested specimens, Equation (2) is used to evaluate the characteristic length L_{ch}. This length can be used as an index of the brittleness of the tested specimen, where the higher the characteristic length, the lower the brittleness and the much ductile the tested prism is:

$$L_{ch} = \frac{E_c G_F}{ft^2}. \quad (2)$$

Based on the experimental results obtained from the control cylinders of splitting tensile strength and modulus of elasticity, the fracture energy G_F and the characteristic length L_{ch} were calculated for each of the four mixtures associated to the four fiber contents. These calculated results are illustrated in Figure 4.

Figure 4(a) explicitly shows that the fracture energy of the used mixture jumped as 0.5% steel fiber was included, which was 23 times that of the plain specimen. On the other hand, L_{ch} showed significant increase from 256 to 3487 when only 0.5% steel fiber was added to the same mixture as shown in Figure 4(b). The two measurements reflect the significant contribution of the low amount of steel fiber to control brittleness and increase ductility of the tested concrete prisms. The inclusion of 1.0% steel fiber is shown to double the fracture energy compared with the specimens with 0.5%, whereas an extra increase in L_{ch}, by approximately 50%, was gained as the fiber content was increased from 0.5% to 1.0%. This result agrees with results obtained by previous researchers [8, 11]. The inclusion of 1.5% steel led to further increase in the ductility; however, the gain over the 1.0% prisms was approximately 18% in terms of fracture energy and approximately 7% in terms of L_{ch}.

The flexural test curves of the tested prisms with the four different fiber contents are shown in Figures 5 and 6. The load-displacement curves of the tested prisms are shown in Figure 5, whereas Figure 6 presents the relationship between load and the crack mouth opening displacement (CMOD). Figure 6 explicitly shows that the inclusion of steel fibers significantly enhanced the flexural performance of the tested prisms. It also shows that the load carrying capacity was higher for fibrous prisms than those without fiber. Moreover, the load-displacement behavior beyond the first crack was significantly improved by fiber inclusion. The figure also presents the strain-hardening behavior of the specimens with a high fiber content of 1.5% until a 2 mm displacement, after which the load capacity showed continuous decrease. On the other hand, the 1.0% fiber content specimens could withstand strain hardening up to approximately 1 mm, beyond which significant load drop was recorded. Such behavior was not noticed for the specimens containing no fiber or 0.5% fiber. Instead, the load carrying capacity dropped directly after cracking, showing significant deflections and CMOD for lower values of load, as shown in Figures 5 and 6. Similar results were also obtained in previous research [8, 11, 19]. This again reveals the significant contribution of steel fibers in changing the flexural behavior from brittle to more ductile.

The strain hardening of prisms with 1.0% and 1.5% fibers can be attributed to the behavior of the fibers during crack bridging. The close examination of the fracture surface along the crack shows that most fibers along the fracture surface of those prisms were pulled out of the matrix. The higher quantity of fibers led to better distribution of stresses on fibers during the crack bridging, which resulted in higher load capacity with uniform displacement and crack opening until they were pulled out. On the other hand, for the prisms with 0.5% fiber, instead of being pulled out of the concrete matrix, most fibers were broken, which is attributed to the high fiber stresses due to the low number of fibers bridging the crack. Figure 7 shows close examination of the fracture surfaces of the four tested prisms.

5. Test Results of the Reinforced Solid and Hollow Beams

In this section, the flexural behavior of the solid and hollow reinforced concrete beams is discussed. The discussion focuses mostly on the effect of cross-sectional hollowing and fiber content on the cracking and failure type, load-displacement behavior, and ductility of the tested beams.

5.1. Cracking and Failure Behavior. In general, beams with steel fiber exhibited better behavior than those without fiber. All solid fibrous beams failed in flexure, whereas those without fiber exhibited less ductile behavior and failed in flexural-shear cracking. The nominal flexural capacity (M_n) of the SFRC beam is the resultant from the contributions of both reinforcing bars (m_1) and the residual tensile strength produced from fiber bridging (m_2). The ACI 544 [44] proposed the following equation for the calculation of the flexural capacity of singly reinforced fibrous concrete solid beams:

$$M_n = m_1 + m_2, \quad (3)$$

where

$$m_1 = A_s f_s \left(d - \frac{a}{2}\right), \quad (4)$$

$$m_2 = \sigma_t b (h - e)\left(\frac{h}{2} + \frac{e}{2} - \frac{a}{2}\right). \quad (5)$$

The above equations were derived from the stress and strain distributions along the depth of the cross section, as shown in Figure 8.

The behavior of hollow fibrous beams was superior to their corresponding beams without fiber, where the fibrous beams failed in pure flexure, whereas the hollow beams without fibers showed flexural and flexural-shear cracking at failure. Based on the ACI 544-proposed equation, the reduction in the flexural capacity of the hollow beams due to the reduction in their cross-sectional area leads to modifying of Equation (5) to the following equation:

$$m_{2,\text{modified}} = \sigma_t \left[b(h - e) - (b' \times h')\right]\left(\frac{h}{2} + \frac{e}{2} - \frac{a}{2}\right), \quad (6)$$

where b, h, and d are the beam cross-sectional dimensions, b' and h' are the hole dimensions, and e is the distance from the top of the tensile stress block to the upper fiber of the beam, which can be obtained through the strain constitutive relation

$$e = \left[\varepsilon_f + 0.003\right]\frac{C}{0.003}, \quad (7)$$

If a is the depth of the rectangular stress block of the hollow section, then

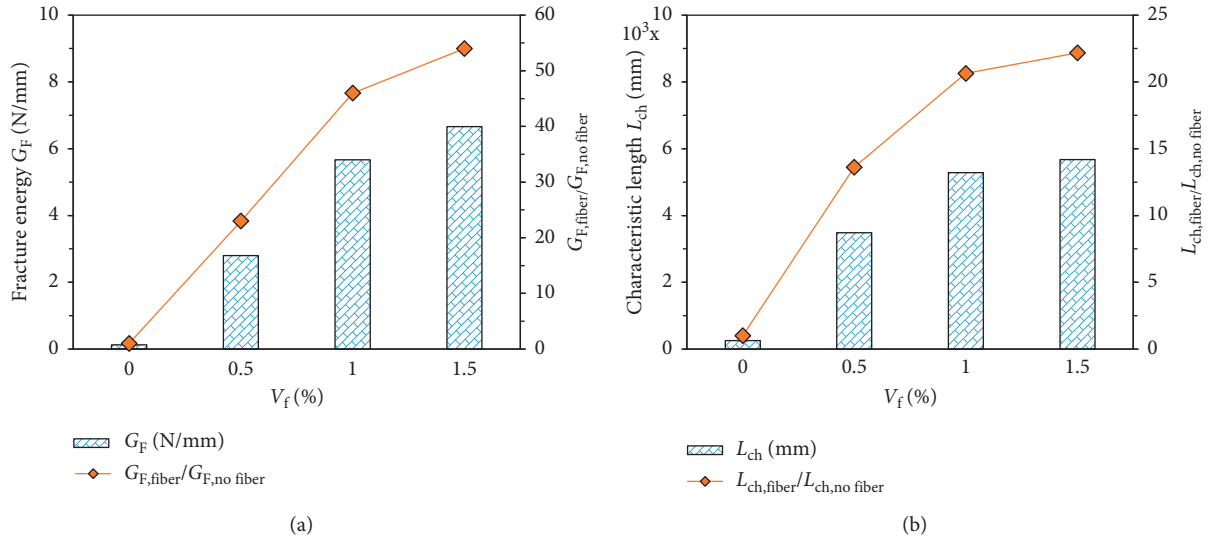

Figure 4: Experimental results of (a) fracture energy G_F and (b) characteristic length L_{ch}.

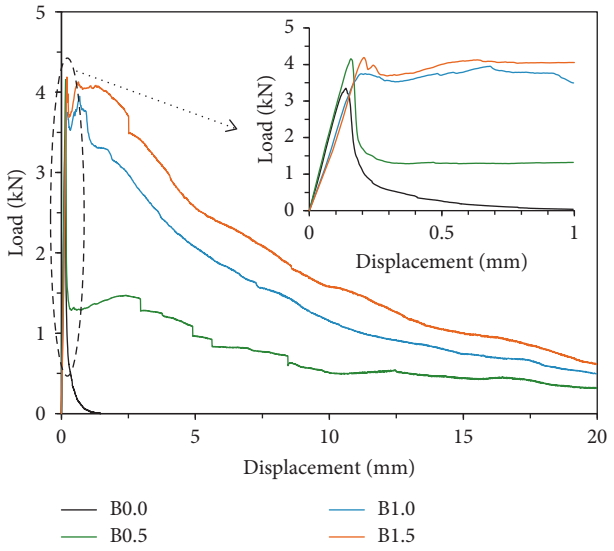

Figure 5: Load-displacement curves of the tested prisms.

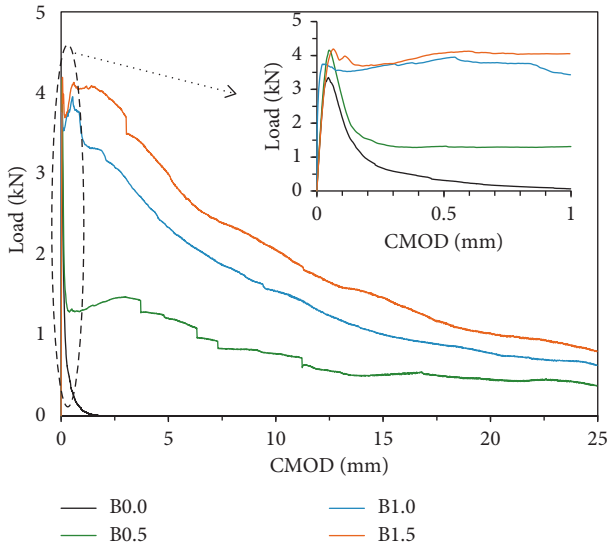

Figure 6: Load-CMOD curves of the tested prisms.

$$a = \frac{A_s f_s + \sigma_t hb - \sigma_t b' h'}{0.85 f'_c b + 512.82 \varepsilon_f \sigma_t b + 1.538 \sigma_t b},$$
$$\sigma_t = 0.00772 \frac{l_f}{d_f} V_f F_{be}, \quad (8)$$

where σ_t is the tensile stress of the fibrous concrete, which is calculated based on the effect of three parameters: the fiber aspect ratio l_f/d_f, the fiber volume fraction (V_f), and the bond between the matrix and the fibers in terms of bond efficiency factor (F_{be}), which is ranging between 1 and 1.2. For the hooked-end steel fiber, F_{be} equals 1.2.

Table 3 summarizes the calculated load capacity based on Equation (3). It shows that the differences between the ultimate loads obtained from the experimental work and the predicted ultimate loads based on ACI 544 are decreasing when increasing the fiber V_f to 6% for 1.5% V_f. On the other hand, these differences are increasing with the increase of V_f for the hollow beams.

Figure 9 shows a cracked beam under bending test. All beams failed by the crushing of the compression concrete after steel yielding and tension crack propagation. As shown in Figure 10, for solid and hollow fibrous beams, flexural vertical cracks were first initiated within the pure moment zone as the applied load reached the cracking load. As the load increased, these crackspropagated and new cracks initiated. The firstly initiated cracks kept propagating until the yielding of the steel reinforcement. After reaching the peak load, compression crushing started to appear in the compression zone of some beams as the load was dropping. In addition to the flexural cracks, flexural-shear cracks

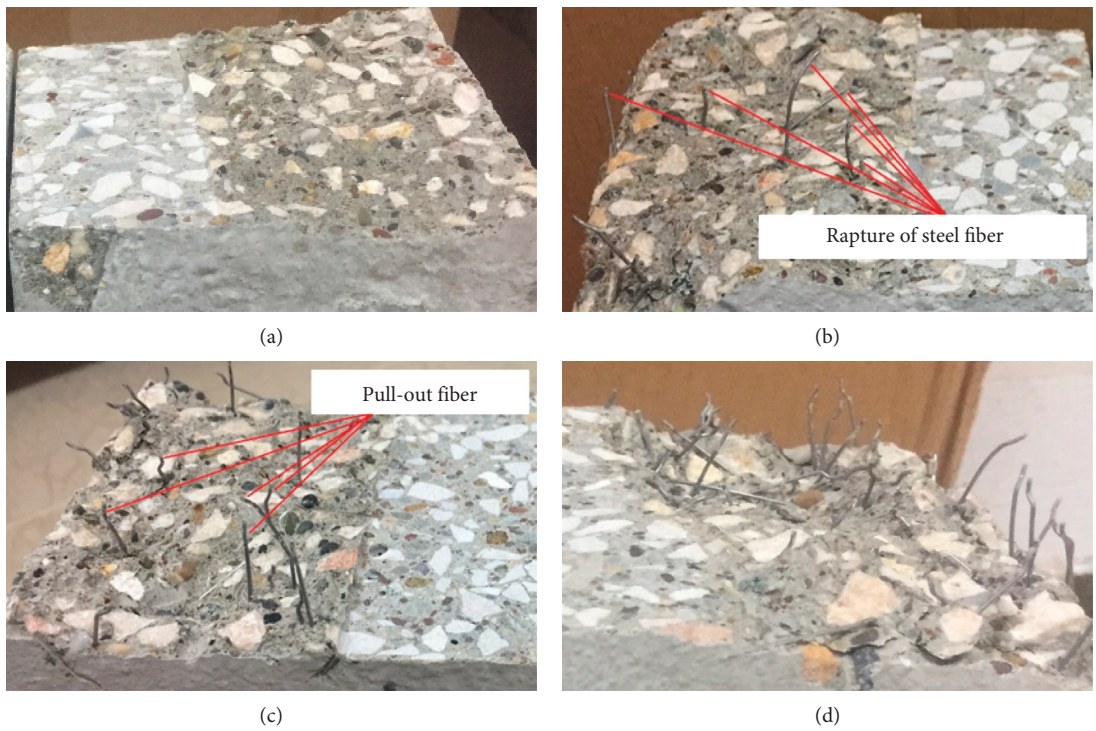

Figure 7: Fracture surfaces of the prisms with different fiber contents: (a) B0.0, (b) B0.5, (c) B1.0, and (d) B1.5.

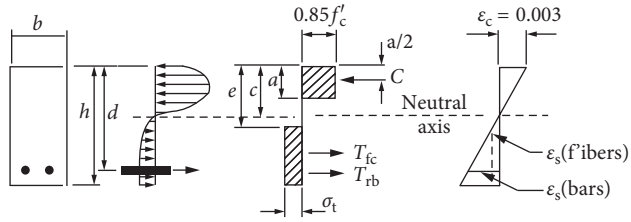

Figure 8: Typical stress and strain distribution in SFRC beams, according to ACI 544.

Table 3: Experimental and predicted results of ultimate load capacity.

Beam ID	h' (mm)	b' (mm)	V_f (%)	P_{u_exp}·(kN)	P_{u_ACI544}·(kN)	P_{u_exp}/P_{u_ACI544}
S-0	0	0	0.0	68.04	54.70	1.24
S-0.5	0	0	0.5	68.92	57.73	1.19
S-1.0	0	0	1.0	71.50	61.17	1.17
S-1.5	0	0	1.5	68.08	64.25	1.06
H-0	80	80	0.0	57.59	54.71	1.05
H-0.5	80	80	0.5	58.90	56.74	1.04
H-1.0	80	80	1.0	69.01	59.16	1.17
H-1.5	80	80	1.5	73.52	61.22	1.20

developed in the beams containing no fibers (S-0 and H-0), as shown in Figure 10. The failure of these two beams was due to the propagation of these cracks outside within the shear span.

5.2. Load-Displacement Curves. Figure 11(a) compares the load-deflection curves of the four solid beams. It is clear in the figure that the yielding load increases as the fiber content increases. The yielding load of the solid beams S-0, S-0.5, S-1.0, and S-1.5 with fiber contents 0, 0.5, 1.0, and 1.5% were 55.4, 57.1, 60.7, and 64.8 kN, respectively. It was also observed that the higher the fiber content, the higher the first cracking load, which reflects the higher potential of fiber reinforced beams to resist the flexural stresses because of the fiber bridging action. The cracking load of the solid beams with fiber contents of 0, 0.5, 1.0, and 1.5% were 21.9, 28.1, 29.5, and 32.7 kN, respectively. The figure also shows that the deflection at steel yielding was less for fibrous beams, which reflects the higher elastic stiffness of steel fiber beams

Figure 9: Tested hollow beam under four-point load.

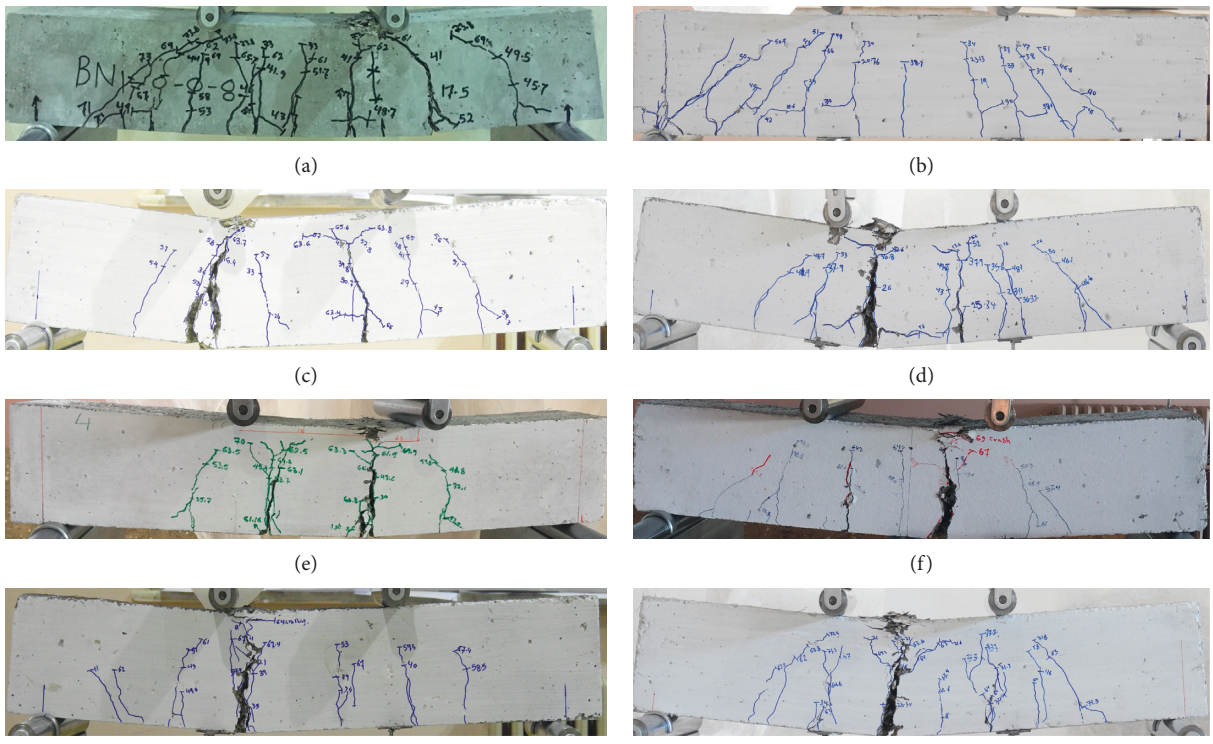

Figure 10: Final cracking patterns of the tested beams after failure: (a) S-0, (b) H-0, (c) S-0.5, (d) H-0.5, (e) S-1.0, (f) H-1.0, (g) S-1.5, and (h) H-1.5.

compared to that without fiber. The recorded deflections at steel yielding were 4.17, 3.51, 3.62, and 2.98 mm for the solid beams S-0, S-0.5, S-1.0, and S-1.5, respectively. This means that the elastic stiffness of the beams increases with the increase in fiber content.

Figure 11(b) clearly clarifies the superior flexural behavior of steel fiber reinforced hollow beams over the ones without steel fiber. It is obvious in the figure that the inclusion of only 0.5% of steel fiber did not lead to significant improvement. However, the inclusion of 1.0 and 1.5% steel fiber is shown to have great impact on the overall structural behavior of hollow beams. The yielding load of the hollow beams H-0, H-0.5, H-1.0, and H-1.5 that contains 0, 0.5, 1.0, and 1.5% steel fiber were 50.3, 46.6, 56.9, and 63.4, respectively. Their corresponding yielding deflections were 3.72, 3.41, 3.39, and 3.36 mm, respectively. This means that the elastic stiffness was almost equal for H-0 and H-0.5, whereas it was 24 and 40% higher for H-1.0 and H-1.5 compared to H-0. Another obvious result is that the higher the fiber content, the higher the peak load the hollow beams could withstand. Similarly, the final deflection (ultimate deflection at failure) was obviously increasing with the

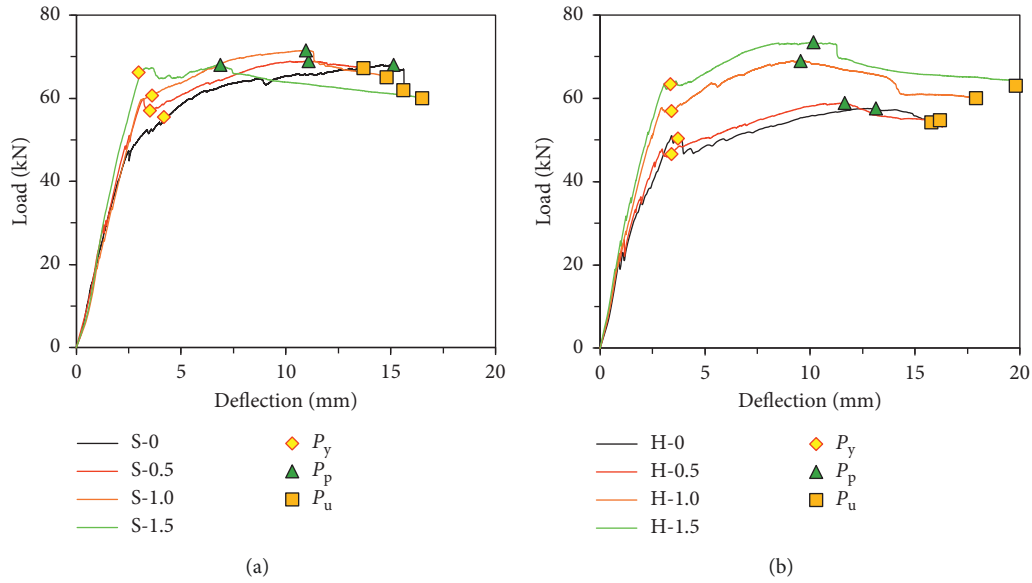

Figure 11: Effect of steel fiber content on load-deflection curves for (a) solid beams and (b) hollow beams.

increase in fiber content in hollow beams, as shown in Figure 11(b). The peak loads of the beams with fiber contents of 0, 0.5, 1.0, and 1.5% were recorded to be 57.6, 58.9, 69.0, and 73.5 kN, respectively, whereas their ultimate deflections were approximately15.8, 16.2, 17.9, and 19.8 mm, respectively. From the discussed results and the comparison between Figures 11(a) and 11(b), it can be concluded that the inclusion of steel fiber was more effective on hollow beams than on solid beams.

Figure 12 compares the load-deflection curves of solid and hollow beams having the same volumetric content of steel fiber. Figure 12(a) shows that the solid beam without fiber could retain higher yield and ultimate load capacities than the corresponding hollow beam. It was recorded that the cracking load of the hollow beam was approximately 5% lower than that of the corresponding solid beam, whereas it was 9% and 15% lower at yielding and ultimate load stages, respectively. It should be reminded that both beams exhibited some flexural-shear cracks outside the pure flexural zone and failed in flexural-shear cracking.

Figure 12(b) shows explicitly that the flexural behavior of S-0.5 was superior to that of the corresponding hollow beam H-0.5. Comparing the load capacities of the two beams at cracking, yielding, and peak stages, it was recorded that the load carrying capacity of H-0.5 was 14.5% to 19.5% lower than that of S-0.5. On the other hand, the flexural behavior of the hollow beam with 1.0% fiber content (H-1.0) is quite close to that of the solid beam S-1.0, as shown in Figure 12(c). It is also shown in the figure that the yielding load capacity of H-1.0 is 6.2% lower than that of the beam S-1.0, whereas its peak load was lower by only 3.5% than that of the beam S-1.0.

Figure 12(d) shows that although that the yielding load capacity is slightly higher for the solid beam with 1.5% of steel fiber (S-1.5), the peak load and its corresponding deflection are noticeably higher for the hollow beam H-1.5 than the solid beam S-1.5, which reflects that the differences in flexural behavior between the solid beam and hollow beam are significantly reduced and diminishes when higher steel fiber contents are used. Comparing the displacement behaviors of the solid and hollow beams in the four figures, it can also be noticed that the length of the strain hardening and softening regions are almost identical for solid and hollow beams, except for the 1.5% fiber content beams, where the hollow beam exhibited noticeably longer strain hardening region.

5.3. Deflection Ductility. The ductility of a reinforced beam under flexural loading can be defined as the capacity of that beam to maintain higher plastic deformations and considerable loads beyond steel yielding until failure without showing sudden brittle fracture [17]. The higher the ductility index, the more ductile is the beam. Previous researchers tried several ductility indices to express the most reasonable representation for ductility. Some researchers used the peak deflection, which is associated to the highest load resisted by the beam, while others used the ultimate deflection, which correspond to the failure load.

Several procedures were proposed by Park [45] to evaluate the ultimate point (Δ_u) from the load-deflection curve of a tested beam. One of these methods is the 20% load reduction after reaching the peak load. Thus, the deflection corresponding to 80% of the peak load on the plastic zone beyond the peak load is considered as the ultimate deflection. Other previous researchers [12, 17] used the 20% load-reduction method to evaluate the ductility of high strength reinforced concrete beams. In the current experimental work, it was noticed that the ultimate failure occurs by concrete crushing very close to the 80% of the peak load or beyond which the load-deflection curve becomes unstable. Therefore, the 20% load-reduction method was also used in this study to obtain the ultimate deflection.

In this study, to evaluate the more reliable ductility index, two ductility indices were calculated based on the

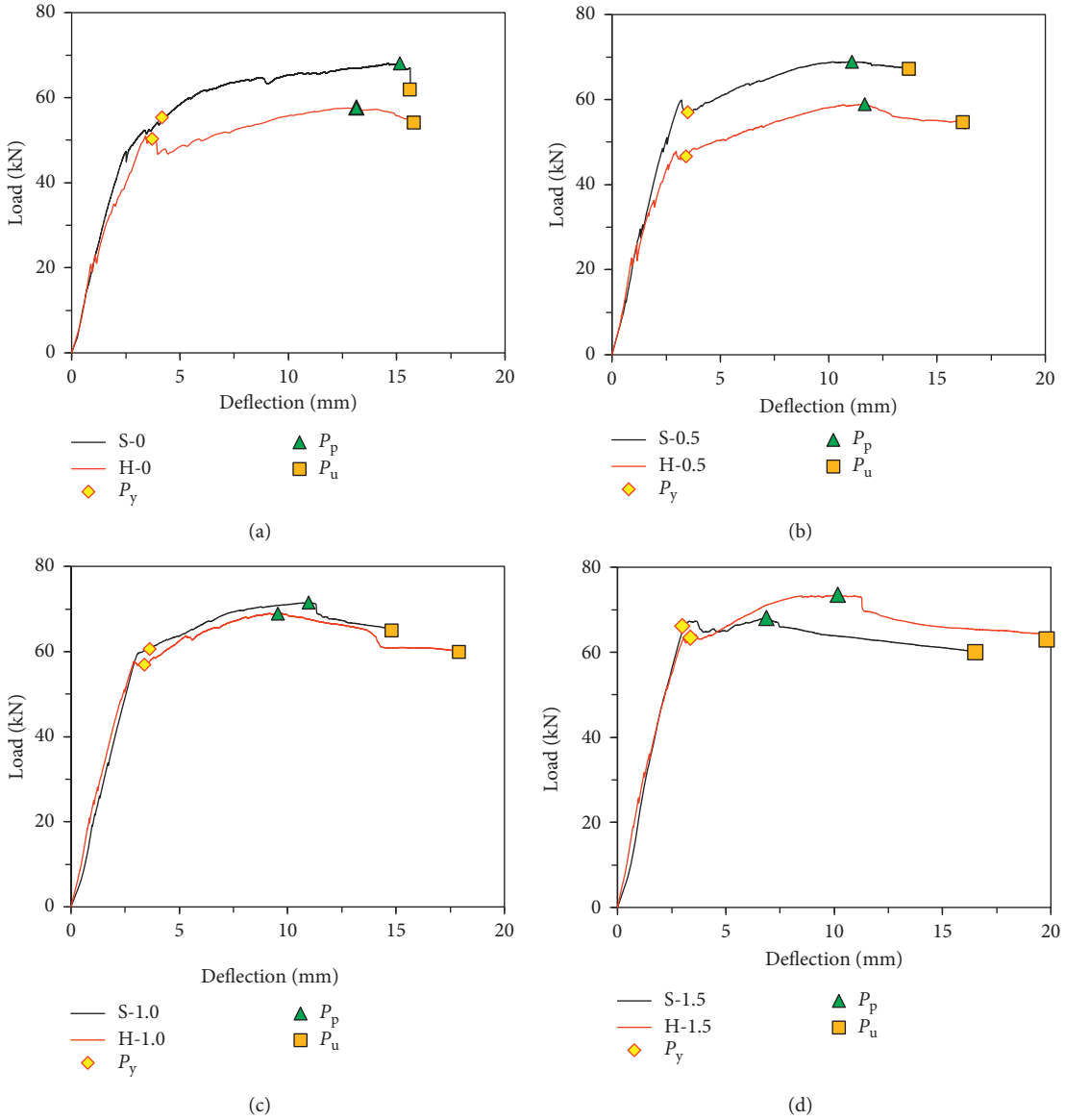

Figure 12: Comparison between load-deflection curves of solid and hollow beams for different fiber contents.

recorded deflections at the yielding of steel (Δ_y), at the peak load (Δ_p), and at the ultimate load (Δ_u). The first ductility index is the peak ductility index (μ_p) calculated at the peak stage and equals Δ_p/Δ_y, whereas the second is the ultimate ductility index (μ_u), which is calculated at the ultimate stage (Δ_u/Δ_y). The values of the three deflections and the two ductility indices are listed in Table 4. Comparing the two calculated ductility indices, it is shown that there is no noticeable trend of ductility with fiber content when μ_p is considered, whereas the results of the ultimate ductility index (μ_p) are systematic with clear trend and agree with the results obtained in the literature [12, 17]. Therefore, in the following discussion, only μ_u is used and is termed simply as ductility index. It was reported in the literature that ductility index of not less than 3 is required for structures constructed in high-seismic zones [17]. It can be seen in Table 3 that all the tested beams exhibited ductility index higher than 3.7, which reflects a high potential to absorb plastic energies when subjected to high loading regimes.

The ductility index values of the four solid beams show that the higher the fiber content, the higher the ductility index. Similarly, comparison among the four hollow beams show that ductility increases as fiber content increases. Figure 13 shows the percentage increase in ductility index of fibrous solid beams and hollow beams compared to the nonfibrous solid beam (S-0). The figure shows that, for solid beams, percentage increases of approximately 4 and 9% were achieved when 0.5 and 1.0% fiber contents, respectively, were incorporated, whereas the percentage increase jumped to approximately 48% when 1.5% steel fiber was used. On the other hand, it is clear that the percentage increases of 27, 41, and 57% were recorded for the hollow beams that contain 0.5, 1.0, and 1.5% steel fiber, respectively. This means that the inclusion of steel fiber enhanced the ductility of reinforced

Table 4: Ductility indices of the solid and hollow tested beams.

Beam ID	Δ_y (mm)	Δ_p (mm)	Δ_u (mm)	$\mu_p = \Delta_p/\Delta_y$	$\mu_u = \Delta_u/\Delta_y$
S-0	4.17	15.14	15.60	3.63	3.74
S-0.5	3.51	13.15	13.70	3.75	3.90
S-1.0	3.62	10.96	14.80	3.03	4.08
S-1.5	2.98	6.88	16.50	2.31	5.54
H-0	3.72	13.15	15.78	3.53	4.24
H-0.5	3.41	11.65	16.20	3.41	4.75
H-1.0	3.39	9.55	17.90	2.82	5.28
H-1.5	3.36	10.16	19.80	3.02	5.89

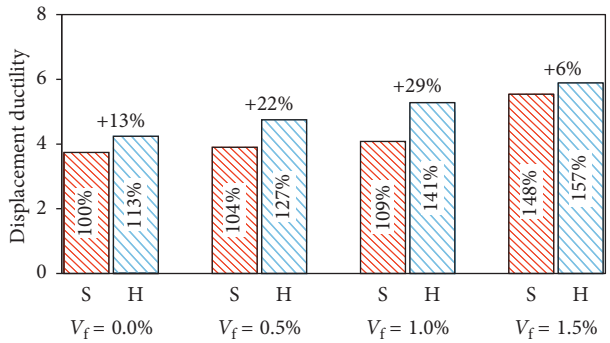

Figure 13: Percentage increase in ductility due to steel fiber inclusion.

concrete beams, and that the maximum percentage increase was achieved when 1.5% steel fiber was used. In the presence of fibers, the firstly initiated cracks are restricted by the bridging action of fibers across that crack, which reduces the crack width and leads to the formation of more hair cracks. Thus, the crack propagation is restricted, which increases the load capacity within the postcracking region. Therefore, the ability of the beam to absorb plastic deformations is increased. Sun et al. [20] reported that the ductility was increased as steel fiber content increased up to 1.5%, beyond which no ductility gain was recorded. It is known that there should be some optimum content of fibers, beyond which, no further enhancement in strength or performance is obtained. The optimum content depends mainly on the fiber physical characteristics [13]. In this research, and within the limit of the studied variables, the 1.5% volumetric content was found to better enhance the load carrying capacity, stiffness, and deflection.

It is obvious in Figure 13 that hollow beams exhibited higher ductility compared to the solid beam S-0, as discussed before or as compared to the corresponding solid beams having the same fiber content. The percentage shown above each twin of the bar charts in Figure 13 refers to the percentage gain of ductility index of each hollow beam over its corresponding solid beam. It is shown that considerable ductility gains of 6 to 29% were obtained for the hollow beams compared with solid beams. This is a very encouraging result as the side length of the hole was more than half the side length of the beam's cross section. Thus, although the beam cross-sectional area and hence its weight was reduced by 28%, higher ductility was retained.

6. Conclusions

From the experimental work of this study on hollow and solid steel fiber-reinforced high-strength concrete beams, following are the most important conclusions:

(1) All solid and hollow fibrous beams failed in flexure and exhibited flexural cracks along the pure bending span, whereas those without steel fiber showed some cracks within the shear spans in addition to the flexural cracks and exhibited flexural-shear failure.

(2) In general, the flexural behavior of fibrous beams was superior to that of beams without fiber because of the crack bridging action of fibers. The cracking, yielding, and peak load capacities increased due to the incorporation of steel fibers both for solid and hollow beams. The better enhancement in load carrying capacity was mostly recorded for the 1.5% fiber content. For both solid and hollow beams, the gain of the beams with 1.5% fiber over those without fiber in cracking, yielding, and peak loads were in the ranges of approximately 24 to 49%, 17 to 26%, and less than 1.0 to 28%, respectively. Moreover, it was recorded that the higher the fiber content, the higher is the stiffness of the beam.

(3) The hollow beams with fiber contents of 0, 0.5, and 1.0% were observed to withstand lower loads at cracking, yielding, and peak stages than their corresponding solid beams, whereas this was not the case for the 1.5% fiber hollow beam which exhibited higher peak load carrying capacity than its corresponding solid beam.

(4) In general, all tested beams exhibited ductility indices higher than 3.7. However, hollow beams exhibited better ductility than solid beams, showing higher ductility index values. The ductility index for each type of beam increased as the fiber content increased. The ductility index values of solid beams ranged from 3.7 to 5.5, whereas those of hollow beams were in the range of 4.2 to 5.9.

Data Availability

The data used to support the findings of this study are available from the corresponding author upon request.

Conflicts of Interest

The authors declare that they have no conflicts of interest.

References

[1] F. F. Wafa and S. A. Ashour, "Mechanical properties of high-strength fiber reinforced concrete," *ACI Material Journal*, vol. 89, no. 5, pp. 449–454, 1992.

[2] P. S. Song and S. Hwang, "Mechanical properties of high-strength steel fiber-reinforced concrete," *Construction and Building Materials*, vol. 18, no. 9, pp. 669–673, 2004.

[3] J. Thomas and A. Ramaswamy, "Mechanical properties of steel fiber-reinforced concrete," *Journal of Materials in Civil Engineering*, vol. 19, no. 5, pp. 385–392, 2007.

[4] M. Sahmaran and I. O. Yaman, "Hybrid fiber reinforced self-compacting concrete with a high-volume coarse fly ash," *Construction and Building Materials*, vol. 21, no. 1, pp. 150–156, 2007.

[5] W. Abbass, M. I. Khan, and S. Mourad, "Evaluation of mechanical properties of steel fiber reinforced concrete with different strengths of concrete," *Construction and Building Materials*, vol. 168, pp. 556–569, 2018.

[6] B. Li, L. Xu, Y. Shi, Y. Chi, Q. Liu, and C. Li, "Effects of fiber type, volume fraction and aspect ratio on the flexural and acoustic emission behaviors of steel fiber reinforced concrete," *Construction and Building Materials*, vol. 181, pp. 474–486, 2018.

[7] R. V. Balendran, F. P. Zhou, A. Nadeem, and A. Y. T. Leung, "Influence of steel fibres on strength and ductility of normal and lightweight high strength concrete," *Building and Environment*, vol. 37, no. 12, pp. 1361–1367, 2002.

[8] M. Pajak and T. Ponikiewski, "Flexural behavior of self-compacting concrete reinforced with different types of steel fibers," *Construction and Building materials*, vol. 47, pp. 397–408, 2013.

[9] D.-Y. Yoo, N. Banthia, J.-M. Yang, and Y.-S. Yoon, "Size effect in normal- and high-strength amorphous metallic and steel fiber reinforced concrete beams," *Construction and Building Materials*, vol. 121, pp. 676–685, 2016.

[10] A. Venkateshwaran, K. H. Tan, and Y. Li, "Residual flexural strengths of steel fiber reinforced concrete with multiple hooked-end fibers," *Structural Concrete*, vol. 19, no. 2, pp. 352–365, 2017.

[11] D.-Y. Yoo, Y.-S. Yoon, and N. Banthia, "Predicting the post-cracking behavior of normal- and high-strength steel-fiber-reinforced concrete beams," *Construction and Building Materials*, vol. 93, pp. 477–485, 2015.

[12] D. Al-Ghamdy, J. Wight, and E. Tons, "Flexural toughness of steel fiber reinforced concrete," *Journal of King Abdulaziz University-Engineering Sciences*, vol. 6, no. 1, pp. 81–97, 1994.

[13] R. B. Abdul-Ahad and O. Q. Aziz, "Flexural strength of reinforced concrete T-beams with steel fibers," *Cement and Concrete Composites*, vol. 21, no. 4, pp. 263–268, 1999.

[14] S. A. Ashour, F. F. Wafa, and M. I. Kamal, "Effect of the concrete compressive strength and tensile reinforcement ratio on the flexural behavior of fibrous concrete beams," *Engineering Structures*, vol. 22, no. 9, pp. 1145–1158, 2000.

[15] H. J. Pam, A. K. H. Kwan, and M. S. Islam, "Flexural strength and ductility of reinforced normal-and high-strength concrete beams," *Structures*, vol. 146, no. 4, pp. 381–389, 2001.

[16] L. F. A. Bernardo and S. M. R. Lopes, "Neutral axis depth versus flexural ductility in high-strength concrete beams," *Journal of Structural Engineering*, vol. 130, no. 3, pp. 452–459, 2004.

[17] S.-W. Shin, H. Kang, J.-M. Ahn, and D.-W. Kim, "Flexural capacity of singly reinforced beam with 150 MPa ultra high-strength concrete," *Indian Journal of Engineering and Material Sciences*, vol. 17, pp. 414–426, 2010.

[18] F. B. A. Beshara, I. G. Shaaban, and T. S. Mustafa, "Nominal flexural strength of high strength fiber reinforced concrete beams," *Arabian Journal for Science and Engineering*, vol. 37, no. 2, pp. 291–301, 2012.

[19] D.-Y. Yoo, Y.-S. Yoon, and N. Banthia, "Flexural response of steel fiber reinforced concrete beams: effect of strength, fiber content, and strain rate," *Cement and Concrete Composites*, vol. 64, pp. 84–92, 2015.

[20] M. Sun, J. Zhu, N. Li, and C. C. Fu, "Experimental research and finite element anaysis on mechanical property of SFRC T-beam," *Advances in Civil Engineering*, vol. 2017, Article ID 2721356, 8 pages, 2017.

[21] H.-L. Zhang and C.-C. Pei, "Flexural properties of steel fiber types and reinforcement ratio for high-strength recycled concrete beams," *Advances in Structural Engineering*, vol. 20, no. 10, pp. 1512–1522, 2017.

[22] J. Qi, J. Wang, and Z. J. Ma, "Flexural response of high-strength steel-ultra-high-performance fiber reinforced concrete beams based on a mesoscale constitutive model: experimental and theory," *Structural Concrete*, vol. 19, no. 3, pp. 719–734, 2018.

[23] I.-H. Yang, C. Joh, and K.-C. Kim, "A comparative experimental study on flexural behavior of high-strength fiber-reinforced concrete and high-strength concrete beams," *Advances in Material Science and Engineering*, vol. 2018, article 7390798, 13 pages, 2018.

[24] S. R. Abid, A. H. Nahhab, H. K. Al-aayedi, and A. M. Nuhair, "Expansion and strength properties of concrete containing contaminated recycled concrete aggregate," *Case Studies in Construction Materials*, vol. 9, pp. 1–14, 2018.

[25] J. Katzer, "Strength performance comparison of mortars made with waste fine aggregate and ceramic fume," *Construction and Building Materials*, vol. 47, pp. 1–6, 2013.

[26] F. Altun, T. Haktanir, and K. Ari, "Experimental investigation of steel fiber reinforced concrete box beams under bending," *Materials and Structures*, vol. 39, no. 4, pp. 491–499, 2006.

[27] A. Murugesan and A. Narayanan, "Influence of a longitudinal circular hole on flexural strength of reinforced concrete beams," *Practice Periodical on Structural Design and Construction*, vol. 22, no. 2, pp. 1–10, 2017.

[28] A. Murugesan and A. Narayanan, "Deflection of reinforced concrete beams with longitudinal circular hole," *Practice Periodical on Structural Design and Construction*, vol. 23, no. 1, pp. 1–15, 2018.

[29] F. H. Arna'ot, A. A. Abbass, A. A. Abualtemen, S. R. Abid, and M. Özakça, "Residual strength of high strength concentric column-SFRC flat plate exposed to high temperatures," *Construction and Building Materials*, vol. 154, pp. 204–218, 2017.

[30] S. Jang and H. Yun, "Combined effects of steel fiber and coarse aggregate size on the compressive and flexural toughness of high-strength concrete," *Composite Structures*, vol. 185, pp. 203–211, 2018.

[31] J. Katzer and J. Domski, "Quality and mechanical properties of engineered steel fibres used as reinforcement for concrete," *Construction and Building Materials*, vol. 34, pp. 243–248, 2012.

[32] J. Katzer, "Median diameter as a grading characteristic for fine aggregate cement composite designing," *Construction and Building Materials*, vol. 35, pp. 884–887, 2012.

[33] J. P. Zhang, L. M. Liu, Z. D. Zhu, F. T. Zhang, and J. Z. Cao, "Flexural fracture toughness and first-crack strength tests of steel fiber-silica fume concrete and its engineering applications," *Strength of Materials*, vol. 50, no. 1, pp. 166–175, 2018.

[34] M. Nili and V. Afroughsabet, "Combined effect of silica fume and steel fibers on the impact resistance and mechanical properties of concrete," *International Journal of Impact Engineering*, vol. 37, no. 8, pp. 879–886, 2010.

[35] X. H. Wang, S. Jacobsen, S. F. Lee, J. Y. He, and Z. L. Zhang, "Effect of silica fume, steel fiber and ITZ on the strength and fracture behavior of mortar," *Materials and Structures*, vol. 43, no. 1-2, pp. 125–139, 2010.

[36] RILEM TC-50 FMC Recommendation, "Determination of the fracture energy of mortar and concrete by means of three-

point bend test on notched beams," *Materials & Structures*, vol. 18, no. 4, pp. 287–290, 1985.

[37] G. N. J. Kani, "The riddle of shear failure and its solution," *Journal of the American Concrete Institute*, vol. 61, no. 28, pp. 441–467, 1964.

[38] ASTM C1609-12, *Standard Test Method for Flexural Performance of Fiber-Reinforced Concrete (Using Beam with Third-Point Loading*, ASTM International, West Conshohocken, PA, USA, 2012.

[39] ASTM C1018-97, *Standard Test Method for Flexural Toughness and First-Crack Strength of Fiber-Reinforced Concrete (Using Beam with Third-Point Loading)*, ASTM International, West Conshohocken, PA, USA, 1997.

[40] ASTM C1399-10, *Standard Test Method for Obtaining Average Residual-Strength of Fiber-Reinforced*, ASTM International, West Conshohocken, PA, USA, 2010.

[41] A. Conforti, G. Tiberti, and G. A. Plizzari, "Splitting and crushing failure in FRC elements subjected to a high concentrated load," *Composites Part B: Engineering*, vol. 105, pp. 82–92, 2016.

[42] V. Savino, L. Lanzoni, A. M. Tarantino, and M. Viviani, "Simple and effective models to predict the compressive and tensile strength of HPFRC as the steel fiber content and type changes," *Composites, Part B: Engineering*, vol. 137, pp. 153–162, 2017.

[43] B. W. Xu and H. S. Shi, "Correlations among mechanical properties of steel fiber reinforced concrete," *Construction and Building Materials*, vol. 23, no. 12, pp. 3468–3474, 2009.

[44] ACI Committee 544, *Design Considerations for Steel Fiber Reinforced Concrete: Manual of Concrete Practice*, ACI 544–88, Farmington Hills, MI, USA, 1988.

[45] R. Park, "Ductility evaluation from laboratory and analytical testing," in *Proceedings of the 9th World Conference on Earthquake Engineering*, pp. 605–616, Tokyo-Kyoto, Japan, 1988.